J Neurol (2013) 260:2744–2753
DOI 10.1007/s00415-013-7048-2

ORIGINAL COMMUNICATION

Cerebral FDG-PET and MRI findings in autoimmune limbic encephalitis: correlation with autoantibody types

Annette Baumgartner · Sebastian Rauer · Irina Mader · Philipp T. Meyer

Received: 11 May 2013 / Revised: 6 July 2013 / Accepted: 12 July 2013 / Published online: 31 July 2013

Abstract In parallel to the detection of new neuronal autoantibodies, the diagnosis of non-infectious limbic encephalitis has risen. Given that cerebral imaging studies show highly variable results, the present retrospective study investigates imaging findings in association with autoantibody type. An institutional database search identified 18 patients with non-infectious limbic encephalitis who had undergone [18F] fluorodeoxyglucose positron emission tomography (FDG-PET). Sixteen of these patients also underwent magnetic resonance imaging (MRI). MRI and FDG-PET images were categorized as follows: normal (0); mesiotemporal abnormality (1); normal mesiotemporal finding but otherwise abnormal (2). Neuronal autoantibodies were determined in serum and/or CSF. Autoantibodies were grouped according to the cellular localization of their target antigen: antibodies against surface antibodies (i.e., VGKC, NMDAR): 9; antibodies against intracellular antigens (i.e., Hu, Ri, GAD): 4; no autoantibodies: 5. The fraction of abnormal scans was lower for MRI (10/16) than for FDG-PET (14/18). There was a significant association between PET findings and autoantibody type: All patients with autoantibodies against intracellular antigens showed mesiotemporal findings on FDG-PET. In turn, only 2/9 patients with autoantibodies against surface antigens displayed mesiotemporal hypermetabolism. In the remaining seven patients, four scans were rated as normal and three only showed findings outside the mesiotemporal region. A similar association was found using MRI, although this did not reach statistical significance. Autoantibody type was found to be associated with FDG-PET and, to a lesser extent, with MRI imaging results. Our observations may explain the heterogeneity of imaging data in LE and based on in vivo findings support the assumption of different patho mechanisms underlying LE due to antibodies against surface and intracellular antigens, respectively.

Keywords Limbic encephalitis · Cerebral MRI · FDG-PET · Autoimmune antibodies

Introduction

The diagnosis of non-infectious, autoimmune-mediated limbic encephalitis (LE) is generally based on clinical symptoms as well as the detection of specific anti-neuronal autoantibodies. LE-specific traits can also be detected in cerebrospinal fluid (CSF), or by electroencephalography (EEG), cerebral magnetic resonance imaging (MRI) and [^{18}F]fluorodeoxyglucose positron emission tomography (FDG-PET).

A variety of imaging findings have been described for LE, with most studies using MRI to demonstrate regions of hyperintensity in the limbic system on fluid-attenuated inversion recovery (FLAIR) images [1–3]. Moreover, in the last few years, several case reports have described imaging findings in extra limbic areas such as the frontal or parietal cortices [4–9], the cerebellum [8, 10] and

A. Baumgartner (✉) · S. Rauer
Department of Neurology, Albert Ludwigs University Freiburg, Breisacher Str. 64, 79106 Freiburg, Germany
e-mail: annette.baumgartner@uniklinik-freiburg.de

I. Mader
Department of Neuroradiology, University of Freiburg, Freiburg, Germany

P. T. Meyer
Department of Nuclear Medicine, University of Freiburg, Freiburg, Germany

brainstem [10], while others reported normal MRI findings [5, 11–16]. In case series, the occurrence of pathological findings varies widely, ranging from less than 10 % [17] to 100 % [3]. In addition to MRI, whole body FDG-PET is often performed for tumor screening in LE patients, while cerebral FDG-PET may also support the diagnosis of LE. To date, most of the FDG-PET studies (usually case reports) of LE patients describe mesiotemporal hypermetabolism [18–21]. This is often accompanied by hypometabolism in the association cortex, relative metabolic sparing of primary cortices, cerebellum and striatum, with the latter sometimes even appearing hypermetabolic. Nevertheless, with the relatively recent identification of new anti-neuronal autoantibodies, several reports describe distinct, extra-mesiotemporal imaging findings in areas including the cerebellum [8, 11, 12, 16, 22], occipital or frontal regions [4, 13, 22, 23], striatum [24] and thalamus [5, 25], or completely normal FDG-PET scans. As with MRI, no influencing factors have been identified that could explain these highly variable imaging findings. However, it is striking that the diversity of neuropathological findings in LE has increased in proportion to the identification of new autoantibodies, which, in turn, has possibly led to the confirmation of LE in previously unverified cases. To this end, it could be hypothesized that the variability in LE imaging data is due to different auto immunological mechanisms that might be driven by a particular autoantibody type.

The aim of the present study was therefore to investigate the putative association between (1) FDG-PET or (2) MRI findings and autoantibody type. Considering that different pathophysiological principles may be explained on the basis of extracellular versus intracellular localization of the antibody target [26], we chose to pool antibodies into distinct groups comprising those directed against neuronal surface antigens (VGKC, NMDAR) and those directed against intracellular antigens (Hu, Ri, Yo, GAD).

Methods

An institutional database analysis was performed in order to identify patients who had been diagnosed with probable or definitive LE between 2008 and 2011. Only patients who had undergone cerebral FDG-PET were included in this retrospective study. Two neurologists (AB, SR) established the final diagnosis according to published clinical criteria [26–28]; (Table 1). If patients fulfilled all the clinical main criteria (memory deficits of subacute onset, personality changes/psychiatric symptoms of subacute onset and seizures), the diagnosis of LE was confirmed. If patients suffered from only two main symptoms, they had to fulfill at least one of the additional criteria (detection of anti-neuronal autoantibodies in serum or CSF, diagnoses of malignancy, epileptic activity in EEG) in order to be included into the study. If a patient had suffered from seizures, epileptic EEG-activity was not included as a diagnostic criterion. Potential differential diagnoses were excluded by adequate tests. Data were retrospectively analyzed after the patients gave written informed consent (as approved by the local ethics committee of the University Hospital Freiburg, Germany).

Table 1 Clinical criteria: criteria for the diagnosis of limbic encephalitis

Clinical main criteria:
Memory deficits with subacute onset
Personality changes/psychiatric symptoms with subacute onset
Seizures
Additional criteria:
Detection of typical autoantibodies in serum or CSF
Diagnosis of malignancy (concurrent)
Epileptic activity in EEG (only relevant for this classification if the patient did not suffer from seizures)

Patients had to fulfill all clinical main criteria or two clinical main criteria and at least one additional criteria to be included in the present study

Antibody testing

Serum (all patients) or both serum and CSF ($n = 4$) were analyzed in a reference laboratory using an established radioimmunoassay (A. Vincent, Oxford). Additionally, analysis was performed by immunofluorescence on transfected HEK293-cells. Intracellular [Hu, Ri, Yo, cv2/CRMP5, Amphiphysin, Ma1, Ma2, SOX1, GAD, (ravo PNS blot)] and surface [VGKC-complex (LGI1 and CASPR2), GABA B, NMDAR, AMPA1, AMPA2, (Euroimmun)] antibodies were assessed.

Cerebral imaging

MRI was performed using a 12-channel head coil in a whole body scanner at 1.5 T (Magnetom Avanto, Siemens, Erlangen, Germany). The following sequences were acquired: axial T2-weighted (w) and T1w images, coronal T2w fluid-attenuated inversion recovery (FLAIR) images, diffusion-weighted images and ADC maps with a *b*-value of $b = 1{,}000$ s/mm^2 and a contrast-enhanced T1w magnetization-prepared rapid gradient echo (MPRAGE). As all lesions were best detected on FLAIR-weighted images and did not show any diffusion restriction or contrast enhancement, only findings from FLAIR images are reported here.

All cerebral FDG-PET studies were done in conjunction with whole-body PET scans (in search of malignancies;

brain scan first). Following FDG injection and uptake under euglycemic (overnight fasting), standardized resting conditions (eyes open, reduced ambient noise), FDG-PET scans were acquired either on a ECAT EXACT 922/47 stand-alone PET scanner (Siemens-CTI, USA; $n = 9$; 20 min 2D acquisition starting 40 min *p.i.* of 351 ± 43 MBq FDG) or a Gemini TF 64 PET/CT scanner (Philips, The Netherlands; $n = 9$; 10 min 3D acquisition starting 50 min *p.i.* of 280 ± 62 MBq FDG). Brain PET datasets were reconstructed either by filtered back-projection (ECAT scanner; Shepp filter, kernel = 5 mm FWHM; resulting voxel-size = 2.24 × 2.24 × 3.375 mm^3) or by LOR-RAMLA (line of response—row action maximum likelihood expectation algorithm) 3D iterative reconstruction (Gemini TF scanner; number of iterations = 2, relaxation parameter = 0.035, 3D spherically-symmetric Kaiser–Bessel basis functions, blob-shape-alpha = 6.3716, blob-radius = 2.8, blob-grid-size = 2.0375; resulting voxel-size = 2.0 × 2.0 × 2.0 mm^3; i.e. default brain reconstruction). Visual readings were performed after automatic anterior–posterior commissure line realignment on transaxial, coronal and sagittal slices spanning the entire brain. In addition, the reader had access to three-dimensional stereotactic surface projections (3D-SSP) depicting each individual's cerebral FDG uptake and its statistical deviation from age-matched healthy controls. 3D-SSPs were created using the freely available Neurostat/3D-SSP software package (University of Washington, USA) [29]. To compensate for differences in scanner spatial resolution, datasets from the higher-resolution PET/CT systems were smoothed using an isotropic 5 mm Gaussian filter prior to statistical analyses. As demonstrated in a previous study [30], combining the careful reading of standardized PET images with Neurostat/3D-SSP analyses yields highly reproducible results among different readers. Of note, there was no statistically significant association between scanner type and PET imaging findings or autoantibody type (not shown in detail), respectively. Furthermore, no absolute quantification of regional cerebral glucose utilization was pursued. Thus, all reported changes of regional metabolism refer to relative changes.

Cerebral MRI and FDG-PET scans were independently analyzed by a neuroradiologist (IM) and a nuclear medicine specialist (PTM), each of whom has long-standing experience (>10 years) in MRI and PET imaging, respectively. Both investigators were blinded to clinical characteristics and autoantibody status.

All scans were rated for regions of hyperintensity in the hippocampus, amygdala and/or parahippocampal gyrus on FLAIR MRI images (referred to as mesiotemporal abnormalities on MRI), while mesiotemporal hypermetabolism was assessed from the FDG-PET scans. Pathological changes outside the aforementioned regions were also investigated. Depending on the presence of mesiotemporal findings as well as the occurrence of additional imaging findings, all scans were ultimately categorized into one of three groups:

- 0, normal imaging findings.
- 1, mesiotemporal abnormalities with or without pathological findings elsewhere,
- 2, normal mesiotemporal findings, but pathological findings elsewhere.

Of note, mesiotemporal hypermetabolism on FDG-PET is typically accompanied by hypometabolism in the association cortices, with relatively spared metabolism in the primary cortices, striatum and cerebellum.

Statistics

Agreement in findings between MRI and FDG-PET in terms of mesiotemporal abnormalities and final group categorization was assessed with Cohen's kappa and McNemar's test, or Bowker's test of symmetry. The correlation between imaging findings and autoantibody types was explored by Chi-squared tests.

Results

Clinical data

The database search yielded 24 patients who had been clinically diagnosed with LE and investigated by cerebral FDG-PET. Their clinical histories were reviewed by two neurologists (AB, SR) and according to the abovementioned clinical criteria, 18 (10 female, 8 male) of these 24 patients were included in the final analyses (interobserver agreement was 100 %). The diagnosis of LE could not be ascertained in the six excluded patients either because the inclusion criteria were not fulfilled or because potential differential diagnoses could not be completely ruled out. MRI was contraindicated in two of the 18 patients included; therefore, these patients only underwent the standard clinical examination and FDG-PET imaging. The average age (±standard deviation) was 55.3 ± 17.7 years (range: 26–84 years). Autoantibodies against intracellular antigens were found in four patients (Hu $n = 2$, Ri $n = 1$, GAD $n = 1$). Autoantibodies against surface antigens were present in nine patients. Seven of whom were positive for VGKC-complex autoantibodies and three of whom were positive for NMDAR autoantibodies. One patient showed positive results for both NMDAR- and VGKC-complex autoantibodies. In the remaining five patients, no autoantibodies could be detected. Two patients suffered from bronchial carcinoma, one patient from an atypical

carcinoid in the lung, one from melanoma, and one female patient from breast cancer. No malignancy was detected in the remaining 13 patients (Table 2).

In 12 patients, MRI and FDG-PET were performed before immunosuppressive therapy was started. Three patients received prednisolone, two were treated by plasma exchange and one by intravenous immunoglobulin, prednisolone and plasma exchange prior to imaging. The severity of the clinical course had necessitated treatment before imaging; however, in all patients, imaging was performed during acute phase of the disease.

Comparison of MRI and FDG-PET findings

The fraction of abnormal scans was lower for MRI (10/16; 62.5 %) than for FDG-PET (14/18; 77.8 %). However, this difference did not reach statistical significance (McNemar's test for 16 paired examinations, $p = 0.32$) and the overall agreement between MRI and FDG-PET in terms of scan abnormality was moderate (Cohen's kappa = 0.43). Similarly, agreement between these two imaging techniques for mesiotemporal involvement (kappa = 0.38) and overall group categorization (kappa = 0.38) was fair, with no significant difference detected between methods (McNemar's test, $p = 0.65$ and Bowker's test, $p = 0.81$, respectively) (Table 3).

A mesiotemporal pathological finding (i.e. imaging finding group 1; Fig. 1) was detected by MRI and FDG-PET in 8/16 patients (50.0 %) and 10/18 patients (55.6 %), respectively. Two MRI (12.5 %) and four FDG-PET (22.2 %) scans were assigned to group 2 since, despite normal mesiotemporal findings, they exhibited pathological changes; these included hyperintensities in the thalamus and occipital cortex on MRI, and hypometabolism in the thalamus and cortical areas, sometimes accompanied by hypermetabolism in the striatum and cerebellum on FDG-PET (Table 2). Of note, one patient assigned to group 1 by both methods showed very pronounced mesiotemporal hypometabolism and atrophy (with little concomitant hyper intensity) on FDG-PET and MRI, respectively. This finding was interpreted as a postinflammatory defect. The patient suffered from only mild cognitive deficits for about 2 years before these symptoms got worse and additional deficits (ataxia, hemiparesis) occurred. FDG-PET and MRI were prompted by this rather rapid clinical progression. Hence, we assume that the patient initially suffered from a low-grade inflammatory reaction that exacerbated later in the disease course causing a more rapid decline and additional symptoms. In accordance, some case reports describe mesiotemporal hypometabolism in limbic encephalitis several months after symptom onset [1, 18, 31]. The patient suffered from an atypical carcinoid of the lung (detected by whole body PET). A negative [^{11}C] PIB scan excluded concomitant Alzheimer's disease.

Correlation of imaging findings with autoantibody types

All patients with autoantibodies against intracellular antigens showed a mesiotemporal abnormality on FDG-PET ($n = 4$; Fig. 1), whereas only 2/9 patients with autoantibodies against surface antigens displayed mesiotemporal hypermetabolism. In the remaining seven patients, four scans were normal (group 0) and three patients showed pathological metabolic activity in regions exclusively outside the mesiotemporal region (group 2; Figs. 2, 3). FDG-PET imaging in the autoantibody-negative patients showed mesiotemporal hypermetabolism (i.e., group 1) in the majority (4/5) of patients (the remaining patient was categorized as belonging to group 2) (Table 4). There was a significant association between autoantibody type and FDG-PET categorization (Chi-squared test, $p = 0.0195$ including all patients, $p = 0.0149$ after exclusion of autoantibody-negative patients), which was primarily driven by the presence or absence of a pathologic mesiotemporal finding (Chi-squared test, $p = 0.006$ all patients, $p = 0.004$ only autoantibody-positive patients).

MRI findings exhibited a similar, albeit less clear association with autoantibody type: Again, the majority of patients with autoantibodies against intracellular antigens showed mesiotemporal imaging findings (3/4 patients), while the majority of patients with autoantibodies against surface antigens did not (5/8 patients). The scans from autoantibody-negative patients were equally distributed across categories (group 0 and 2, respectively, $n = 1$; group 1, $n = 2$). However, unlike the FDG-PET findings, the association between autoantibody type and MRI findings (overall categorization or presence/absence of limbic findings) was not statistically significant (Chi-squared test, $p > 0.2$ including all or only autoantibody-positive patients).

Discussion

We found a significant association between autoantibody type and FDG-PET findings, with autoantibodies against intracellular antigens being associated with mesiotemporal abnormalities, while autoantibodies against surface antigens were more often associated with either normal findings or abnormalities outside the mesiotemporal region. A similar association was also found with MRI, but this did not reach statistical significance. In support of our results, it is remarkable that nearly all previous studies in which LE

Table 2 Clinical data, serum and CSF content, and EEG, MRI and FDG-PET findings

Pat.	Sex	Age	Clinical main criteria	Additional symptoms	Ab	Malignancy	EEG	FLAIR-MRI			FDG-PET		
								mesiotemporal	Additional findings	Category	Mesiotemporal	Additional findings	Category
1	f	58	√	–	Hu, SOX	SCLC	0	√		1	√	Hypometabolism in association cortices	1
2	m	69		Tetra spastic	VGKC (LQI1)	No	1	√		1	√	Hypometabolism in association cortices (left > right)	1
3	f	71		Gait disturbance	VGKC	No	1		Hydrocephalus (unrelated)	0		Hydrocephalus (unrelated)	0
4	m	26	√	Hypomania, somnolence, hallucinations	VGKC	No	2			0		Pronounced hypometabolism temporoparietooccipital, hypermetabolism in striata and cerebellum	2
5	f	31	√	Dyskinesia, cognitive deficits	NMDA	No	2		Occipital	2		Hypometabolism left hemispheric cortex and thalamus and (less pronounced) right temporal lobe; crossed cerebellar diaschisis (right); hypermetabolism in striata	2
6	f	43		Nausea, hallucinations	GAD	No	0	√		1	√	None	1
7	m	67		Cognitive deficits	VGKC (CASPR2)	No	–			–	√	Hypometabolism in association cortices, hypermetabolism of striata	1
8	f	42	√	Cognitive deficits, disorientation	No	No	1	√	Parietal	1	√	Hypometabolism of association cortices, hypermetabolism in striata and cerebellum	1
9	m	78		Confusion, disorientation, psychomotor retardation	No	No	2		svd	0	√	Mild parietal and left frontal hypometabolism	1
10	f	59	√	Confusion	No	No	1	√		1	√	Hypometabolism in association cortices, hypermetabolism of striata	1
11	m	51		–	VGKC, NMDA	No	2	√	Thalmus and insula	1		Hypometabolism in thalami	2

Table 2 continued

Pat.	Sex	Age	Clinical main criteria	Additional symptoms	Ab	Malignancy	EEG	FLAIR-MRI			FDG-PET		
								mesiotemporal	Additional findings	Category	Mesiotemporal	Additional findings	Category
12	m	61		Disorientation, attention deficits	VGKC (CASPR2)	No	0		svd	0		None	0
13	m	79		Brainstem syndrome	Hu	SCLC	–		svd	0	√	Hypometabolism in association cortices	1
14	f	63		Ataxia, cognitive deficits, mild hemiparesis	Ri	Atypical carcinoid in the lung	–	√*	svd	1	√*	Severe mesiotemporal hypometabolism	1
15	m	84		Confusion	No	Melanoma	0			–		Hypometabolism in thalami, metastasis in cerebellum (unrelated)	2
16	f	42		Amnesic aphasia	No	No	2		Thalamus	2	√	Hypometabolism in association cortices	1
17	f	38		Brainstem syndrome, ataxia	NMDA	Breast cancer	1	√		1		None	0
18	f	33		Mania	VGKC	No	0			0		None	0

Categorization of EEG: 0, normal findings; 1, pathological findings without epileptic activity; 2, epileptic activity. Categorization of MRI and PET finding: 0, normal imaging findings; 1, mesiotemporal abnormality with or without pathological findings elsewhere; 2, other: normal mesiotemporal finding, but pathological findings elsewhere. Of note, mesiotemporal hypermetabolism on FDG-PET (group 1) is typically accompanied by hypometabolism in the association cortices, with relatively spared metabolism in primary cortices, striatum and cerebellum (possibly also increased in the latter two structures)

Ab antibodies, *CSF* cerebrospinal fluid, *EEG* electroencephalography, *m* male, *f* female, *SCLC* small cell lung cancer, *svd* small vessel disease, unrelated to LE

* MRI: pronounced atrophy and hyperintensive signal alteration and, PET: severe mesiotemporal hypometabolism: interpreted as a postinflammatory defect

Table 3 Associations between MRI and FDG-PET findings

		PET findings		
		Group 0	Group 1	Group 2
MRI findings	Group 0	3	2	1
	Group 1	1	6	1
	Group 2	0	1	1
	No MRI	0	1	1

Numbers of patients within each group of imaging findings are given (see "Table 2")

patients displayed hypermetabolism in the mesiotemporal region also reported that these patients were positive for autoantibodies against intracellular antigens [1–3, 31]. Furthermore, most reports on LE patients with autoantibodies against surface antigens describe normal metabolism in mesiotemporal regions, but pathological findings in other cerebral regions [4, 5, 11–13, 15, 22, 24]. In agreement with our data, pathological findings in these patients were often localized in the cerebellum, thalamus and parietal or occipital cortex [8, 17, 22, 23, 32].

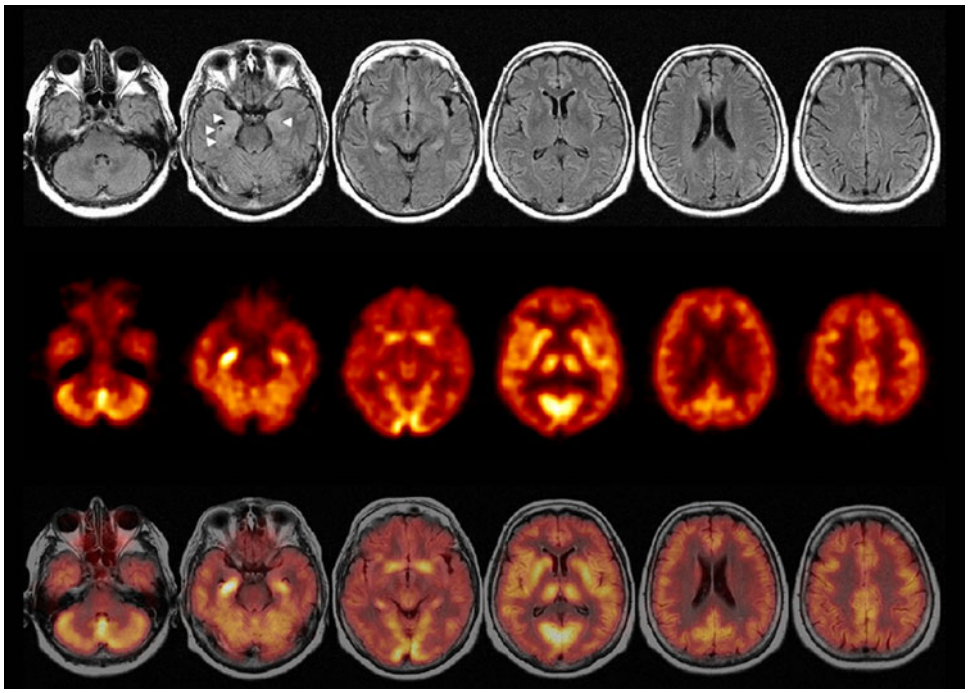

Fig. 1 Representative imaging results in a patient with autoantibodies directed against an intracellular antigen (patient 1). FLAIR MRI (*first row*) depicts bilateral mesiotemporal signal hyperintensities (*arrow heads*), while FDG-PET (*second row*) shows extensive bilateral mesiotemporal hypermetabolism in addition to hypometabolism in the association cortices. *Third row*: PET/MRI fusion images. This patient was categorized into group 1 by both imaging modalities; anti-Hu-antibodies were detected in serum

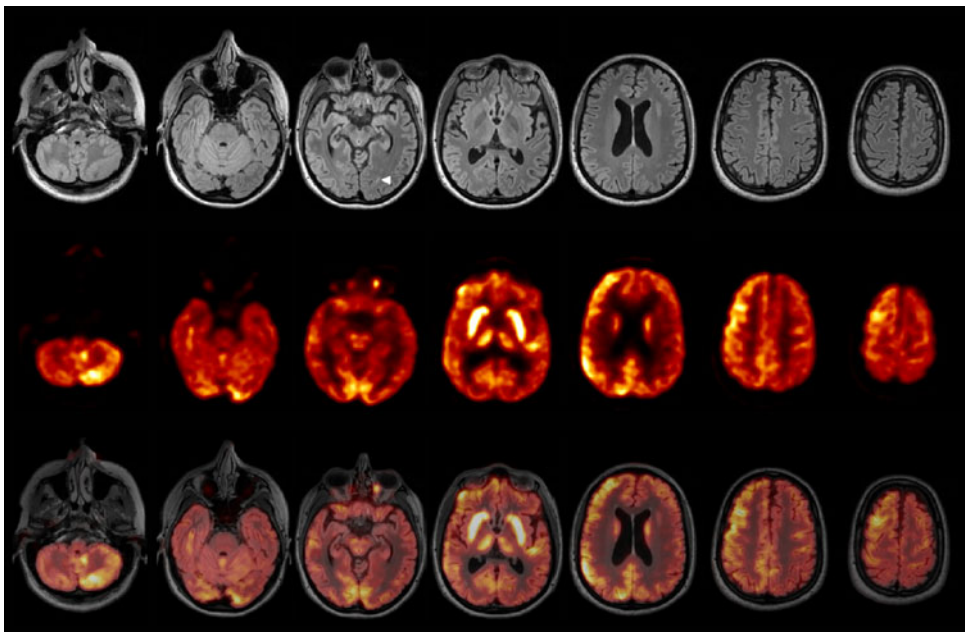

Fig. 2 Imaging results in a patient with autoantibodies directed against the NMDA receptor (patient 5). Whereas only a small occipital signal hyperintensity on FLAIR MRI (*first row*) was evident, FDG-PET (*second row*) depicted extensive hypometabolism in the *left* hemispheric cortex, thalamus, and (less pronounced) *right* temporal lobe. In addition, note the crossed cerebellar diaschisis (*right*) and the hypermetabolism in the bilateral striata. Both scans were categorized into group 2. *Third row*: PET/MRI fusion images

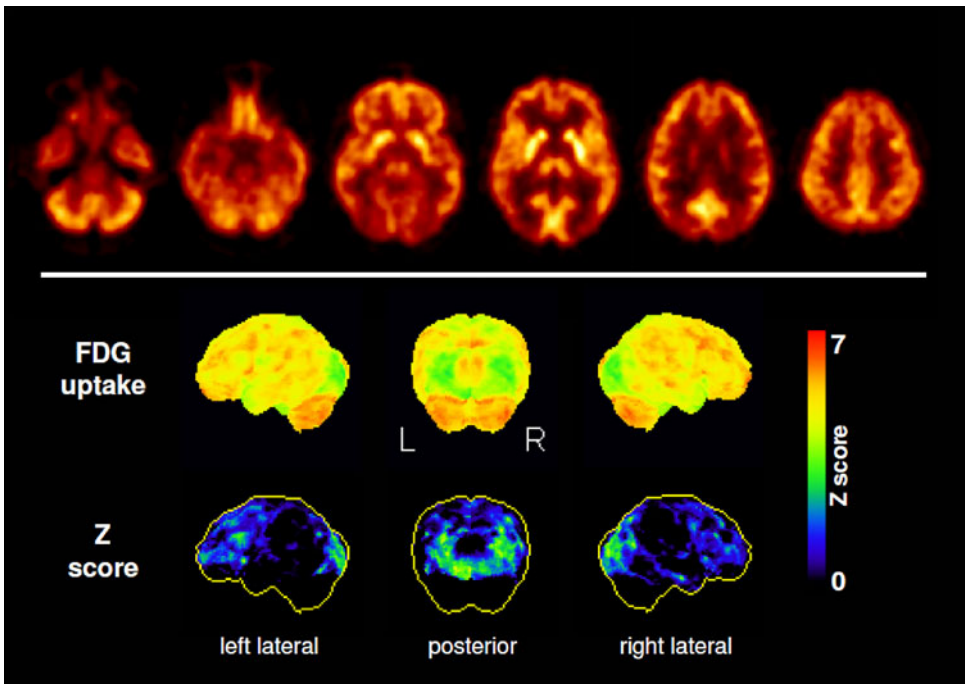

Fig. 3 Results of FDG-PET imaging in a patient with VGKC antibodies (patient 4). *Upper panel*: transaxial FDG-PET images; *lower panel*: three-dimensional stereotactic surface projections of FDG uptake (*first row*) and *Z* score values (*second row*; statistical deviation from a sample of age-matched healthy controls; shown are decreases of FDG uptake). Note the significant hypometabolism of the posterior temporoparietooccipital cortices, while the bilateral striatum and cerebellum show spared metabolism (categorized into group 2). MRI was normal (group 0)

Table 4 Association between imaging findings and autoantibody specificities

	FDG-PET findings			MRI findings		
	Group 0	Group 1	Group 2	Group 0	Group 1	Group 2
Total	4	10	4	6	8	2
Intracellular antibodies	0	4	0	1	3	0
Hu	0	2	0	1	1	0
Ri	0	1	0	0	1	0
GAD	0	1	0	0	1	0
Surface antibodies	4	2	3*	4	3*	1
NMDAR	1	0	2	0	2	1
VGKC	3	2	2	4	2	0
Antibody negative	0	4	1	1	2	1

Numbers of patients within each group of imaging findings are given (see "Table 2") and antibody specificity

* In one patient, both NMDAR and VGKC-antibodies were detectable

These associations might be explained by different effector mechanisms of the underlying autoimmune process on neuronal cells; LE that is associated with autoantibodies against intracellular antigens is presumably caused by a *T*-cell-effector mechanism directed at the limbic system [33]. Cytotoxic *T*-cell processes induce inflammatory tissue damage through a combination of immune cell migration, activation, and the release of cytokine and chemokines. In turn, these inflammatory processes not only promote tissue repair and gliosis, they also increase the energy turnover of affected cells. Given that these mechanisms lead to an increased FDG uptake, our findings support the proposed *T*-cell-mediated patho mechanism in LE associated with antibodies against intracellular antigens.

In contrast, LE that is associated with antibodies against cell surface antigens may be caused by an interaction between a particular antibody and its antigen target, usually a neuronal receptor (e.g., NMDA, VGKC-complex). In line with this, Hughes et al. [34] suggested that a decrease in the surface density of NMDA receptors via antibody-mediated capping and internalization was a probable patho mechanism in NMDAR-positive LE. In addition, LE associated with antibodies against cell surface antigens could be caused by a direct blockade of receptors or ion channels by autoantibodies. Both these patho mechanisms may lead to a

decrease in neuronal activity and, as a consequence, hypometabolism in the affected regions. In addition, both effector mechanisms are not necessarily expected to induce inflammatory cellular damage or general activation of immune cells and tissue repair mechanisms that would cause a relevant increase in glucose metabolism.

Taken together, our data provide the first in vivo evidence for different patho mechanisms underlying LE associated with either antibodies against intracellular or surface antigens.

None of the antibody-negative patients showed normal findings on both MRI and FDG-PET imaging. In particular, four out of five patients showed mesiotemporal hypermetabolism on FDG-PET. It is tempting to speculate that LE in these patients is associated with yet to be identified antibodies that are directed against intracellular antigens or lead to an inflammatory reaction similar to that of known intracellular autoantibodies. Moreover, this also implies that imaging results, particularly those generated by FDG-PET, could make an important contribution to the diagnosis of LE in autoantibody-negative patients.

We found one patient with NMDAR- as well as VGKC-antibodies. To our knowledge, only one other case report exists about a patient being positive for both of these antibodies [35]. Our patient showed typical limbic findings on MRI and extra-limbic pathological metabolism on FDG-PET. It is also interesting that pathological findings in thalamus were exclusively detected in this patient by both imaging techniques.

Considering the sensitivity of both imaging modalities for LE-associated pathological findings, we found a slightly higher sensitivity with FDG-PET (78 %) compared to MRI (63 %), although this difference did not reach statistical significance. Nevertheless, there were only six patients showing typical findings on both cerebral MRI and FDG-PET. Otherwise, in patients with typical mesiotemporal findings on either cerebral MRI or FDG-PET, LE could be detected by at least one of these imaging investigations in 11/16 patients who were investigated by both methods. Hence, examining patients with clinically-suspected LE by both methods could increase the sensitivity of LE diagnosis in clinical practice. Thus, since cerebral MRI imaging is commonly performed in clinical practice, the addition of FDG-PET seems to be a reasonable means of enhancing the sensitivity of the diagnostic algorithm, especially in patients with normal MRI scans. As an additional benefit, whole-body FDG-PET scanning to screen for malignancy can easily be added to the same PET session in which patients undergo screening for suspected paraneoplastic LE.

In summary, we found that autoantibody type showed associations with FDG-PET results and, to a lesser extent, with MRI imaging findings, which may explain the heterogeneity of imaging findings in LE. The present in vivo data support the assumption that different patho mechanisms underlie LE due to antibodies against surface and intracellular antigens, respectively.

However, due to the overall rarity of autoimmune LE, we investigated only a rather small cohort. Future prospective studies are needed.

Acknowledgments The authors thank Dr. Sandra Dieni for helpful comments on the text.

Conflicts of interest A.B and S.R. report receiving consulting and lecture fees, grant and research support from Bayer Vital GmbH, Biogen Idec, Merck Serono, Novartis, Sanofi-Aventis and Teva. S.R. is a founding member of ravo Diagnostika GmbH, Freiburg. I.M. is supported by the German Research Council (DFG MA-2343/41) and by the Bernstein Focus of Neuro technology (B3). P.T.M. received research grants from GE Healthcare and payments for lectures by Siemens AG and consultancy by Bayer-Schering AG. None of the authors has any financial or personal relationships with individuals or organizations that could inappropriately influence this submission.

Ethical standard This study was approved by the local ethic committee and patients gave written informed consent.

References

1. Scheid R, Lincke T, Voltz R et al (2004) Serial 18F-fluoro-2-deoxy-D-glucose positron emission tomography and magnetic resonance imaging of paraneoplastic limbic encephalitis. Arch Neurol 61:1785–1789
2. Provenzale JM, Barboriak DP, Coleman RE (1998) Limbic encephalitis: comparison of FDG-PET and MR imaging findings. Am J Roentgenol 170:1659–1660
3. Hoffmann LA, Jarius S, Pellkofer HL et al (2008) Anti-Ma and anti-Ta associated paraneoplastic neurological syndromes: 22 newly diagnosed patients and review of previous cases. J Neurol Neurosurg Psychia 79:767–773
4. Greiner H, Leach JL, Lee KH et al (2011) Anti-NMDA receptor encephalitis presenting with imaging findings and clinical features mimicking Rasmussen syndrome. Seizure 20:266–270
5. Pillai SC, Gill D, Webster R et al (2010) Cortical hypometabolism demonstrated by PET in relapsing NMDA receptor encephalitis. Pediatr Neurol 43:217–220
6. Prüss H, Dalmau J, Harms L et al (2010) Retrospective analysis of NMDA receptor antibodies in encephalitis of unknown origin. Neurology 75:1735–1739
7. Ishiura H, Matsuda S, Higashihara M et al (2008) Response of anti-NMDA receptor encephalitis without tumour to immunotherapy including rituximab. Neurology 71:1921–1923
8. Vitaliani R, Mason W, Ances B et al (2005) Paraneoplastic encephalitis, psychiatric symptoms, and hypoventilation in ovarian teratoma. Ann Neurol 58:594–604
9. Gultekin SH, Rosenfeld MR, Voltz R et al (2000) Paraneoplastic limbic encephalitis: neurological symptoms, immunological findings and tumour association in 50 patients. Brain 123:1481–1494
10. Dalmau J, Tüzün E, Wu HY et al (2007) Paraneoplastic anti-*N*-methyl-D-aspartate receptor encephalitis associated with ovarian teratoma. Ann Neurol 61:25–36
11. Maqbool M, Oleske DA, Huq AH et al (2011) Novel FDG-PET findings in NMDA receptor encephalitis: a case based report. Child Neurol 26:1325–1328

12. Caballero PE (2011) Fluorodeoxyglucose positron emission tomography findings in NMDA receptor antibody encephalitis. Arq Neuropsiquiatr 69:409–410
13. Padma S, Sundaram PS, Marmattom BV (2011) PET/CT in the evaluation of anti-NMDA-receptor encephalitis: what we need to know as a NM physician. Ind J Nucl Med 26:99–101
14. Haberlandt E, Bast T, Ebner A et al (2011) Limbic encephalitis in children and adolescents. Arch Dis Child 96:186–191
15. Maeder-Ingvar M, Prior JO, Irani SR et al (2011) FDG-PET hyperactivity in basal ganglia correlating with clinical course in anti-NDMA-R antibodies encephalitis. J Neurol Neurosurg Psychia 82:235–236
16. Guenther A, Brodoehl S, Witte OW et al (2012) Atypical post-hypoxic MRI changes in hypermetabolic regions in anti-NMDA-receptor encephalitis. Neurology 79:720–721
17. Irani SR, Bera K, Waters P et al (2010) *N*-methyl-D-aspartate antibody encephalitis: temporal progression of clinical and para clinical observations in a predominantly non-paraneoplastic disorder of both sexes. Brain 133:1655–1667
18. Chatzikonstantinou A, Szabo K, Ottomeyer C et al (2009) Successive affection of bilateral temporomesial structures in a case of non-paraneoplastic limbic encephalitis demonstrated by serial MRI and FDG-PET. J Neurol 256:1753–1755
19. Troester F, Weske G, Schlaudraff E et al (2009) Image of the month. FDG-PET in paraneoplastic limbic encephalitis. Eur J Nucl Med Mol Imag 36:539
20. Ances BM, Vitaliani R, Taylor RA et al (2005) Treatment-responsive limbic encephalitis identified by neuropil antibodies: MRI and PET correlates. Brain 128:1764–1777
21. Kassubek J, Juengling FD, Nitzsche EU et al (2001) Limbic encephalitis investigated by 18 FDG-PET and 3D MRI. J Neuroimag 11:55–59
22. Mohr BC, Minoshima S (2010) F-18 fluorodeoxyglucose PET/CT findings in a case of anti-NMDA receptor encephalitis. Clin Nucl Med 35:461–463
23. Leypoldt F, Buchert R, Kleiter I et al (2012) Fluorodeoxyglucose positron emission tomography in anti-*N*-methyl-D-aspartate receptor encephalitis: distinct pattern of disease. J Neurol Neurosurg Psychia 83:681–686
24. Rey C, Koric L, Guedj E et al (2012) Striatal hypermetabolism in limbic encephalitis. J Neurol 259:1106–1110
25. Malter MP, Helmstaedter C, Urbach H et al (2010) Antibodies to glutamic acid decarboxylase define a form of limbic encephalitis. Ann Neurol 67:470–478
26. Graus F, Delattre JY, Antoine JC, Dalmau J, Giometto B, Grisold W et al (2004) Recommended diagnostic criteria for paraneoplastic neurological syndromes. J Neurol Neurosurg Psychia 75:1135–1140
27. Dalmau J, Gleichman AJ, Hughes EG, Rossi JE, Peng X, Lai M et al (2008) Anti-NMDA-receptor encephalitis: case series and analysis of the effects of antibodies. Lan Neurol 7:1091–1098
28. Vincent A, Bien CG, Irani SR, Waters P (2011) Autoantibodies associated with diseases of the CNS: new developments and future challenges. Lan Neurol 10:759–772
29. Minoshima S, Frey KA, Koeppe RA, Foster NL, Kuhl DE (1995) A diagnostic approach in Alzheimer's disease using three-dimensional stereotactic surface projections of fluorine-18-FDG PET. J Nucl Med 36:1238–1248
30. Hellwig S, Amtage F, Kreft A, Buchert R, Winz OH, Vach W et al (2012) [18F]FDG-PET is superior to [123I]IBZM-SPECT for the differential diagnosis of parkinsonism. Neurology 79:1314–1322
31. Blanc F, Ruppert E, Kleitz C, Valenti MP, Cretin B, Humbel RL et al (2009) Acute limbic encephalitis and glutamic acid decarboxylase antibodies: a reality? J Neurol Sci 287:69–71
32. Fisher RE, Patel NR, Lai EC, Schulz PE (2012) Two different 18F-FDG brain PET metabolic patterns in autoimmune limbic encephalitis. Clin Nucl Med 37:213–218
33. Bien CG, Vincent A, Barnett MH, Becker AJ, Blümcke I, Graus F et al (2012) Immunopathology of autoantibody-associated encephalitides: clues for pathogenesis. Brain 135:1622–1638
34. Hughes EG, Peng X, Gleichman AJ, Lai M, Zhou L, Tsou R et al (2010) Cellular and synaptic mechanisms of anti-NMDA receptor encephalitis. J Neurosci 30:5866–5875
35. Pellkofer HL, Kuempfel T, Jacobson L, Vincent A, Derfuss T (2010) Non-paraneoplastic limbic encephalitis associated with NMDAR and VGKC antibodies. J Neurol Neurosurg Psychia 81:1407–1408